

# Challenges and solutions for high-efficiency quantum dot-based LEDs

Deniz Bozyigit and Vanessa Wood

Colloidal quantum dots (QDs) hold great promise as electrically excited emitters in light-emitting diodes (LEDs) for solid-state lighting and display applications, as highlighted recently by the demonstration of a red-emitting QD-LED with efficiency on par with that of commercialized organic LED technologies. In the past five years, important advances have been made in the synthesis of QD materials, the understanding of QD physics, and the integration of QDs into solid-state devices. Insights from this progress can be leveraged to develop a set of guidelines to direct QD-LED innovation. This article reviews the fundamental causes of inefficiency in QD-LEDs understood to date and proposes potential solutions. In particular, we emphasize the challenge in developing QD emitters that exhibit high luminescent quantum yields in the combined presence of charge carriers and electric fields that appear during traditional LED operation. To address this challenge, we suggest possible QD chemistries and active layer designs as well as novel device architectures and modes of QD-LED operation. These recommendations serve as examples of the type of innovations needed to drive development and commercialization of high-performance QD-LEDs.

## Challenges in QD-LEDs

Colloidal quantum dot (QD)-based light-emitting devices (QD-LEDs) are of considerable interest for applications such as thin-film displays and white lighting with improved and selectable color.<sup>1</sup> One metric for defining the performance of a QD-LED is the external quantum efficiency (EQE), which is the number of photons emitted from the device per injected electron. The red-emitting QD-LED with 18% EQE, recently demonstrated by QD Vision Inc., underscores the potential for QD-LEDs to compete and eventually surpass the efficiency of organic LED (OLED) technology.<sup>2</sup> However, the EQE of most QD-LEDs, particularly those emitting in blue or green, is significantly less.<sup>3,4</sup> Understanding what limits efficiency is critical for the systematic development of QD chemistries and device architectures for high-performance QD-LEDs.

## Efficiency in QD-LEDs

Efficient electron and hole injection, balance of charge carriers arriving at the QD active layer, and minimization of the electric field across the QDs are all important design criteria for ensuring high-performance QD-LEDs.<sup>2,5,6</sup> However, these design guidelines are highly device specific and difficult to achieve in the same device for different color emitters with various chemistries and sizes.<sup>3,6</sup>

Given the extensive discussion of optimization in device structure in prior literature, in this article, we do not consider the challenges of bringing charge carriers to the QD layer and forming excitons on the QDs; rather, we examine efficiency in the last step of the light generation process in a QD-LED. Namely, when an exciton is present on the QD, what is the probability that it will recombine to emit a photon, which can be quantified by the luminescent quantum yield (QY). The device EQE can thus be assumed to be proportional to the QY of the emitters in the device structure, which depends on the exciton nonradiative ( $k_{nr}$ ) and radiative ( $k_r$ ) recombination rates:

$$\text{EQE} \propto \text{QY} = k_r / (k_{nr} + k_r). \quad (1)$$

As illustrated schematically in **Figure 1**,  $k_{nr}$  and  $k_r$  are determined by the QDs themselves and the interaction of the QDs with the electric field (F) and charge (Q) resulting from the voltage and current needed to operate the LED.

In a QD-LED, the two major contributors to the non-radiative rate are electronic trap states and free-charge carriers. For example, if the QD emitter has surface state defects, trap-assisted recombination can occur, whereby the electron or hole in an exciton relaxes to a trap state, and the two carriers subsequently recombine without emission of a photon.<sup>7</sup> This

Deniz Bozyigit, ETH Zürich, Switzerland; denizb@iis.ee.ethz.ch  
Vanessa Wood, ETH Zürich, Switzerland; vwood@ethz.ch  
DOI: 10.1557/mrs.2013.180

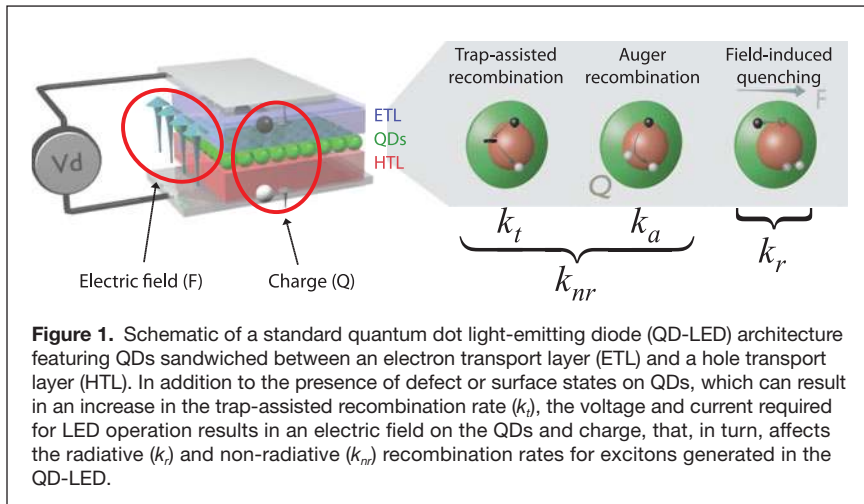


**Figure 1.** Schematic of a standard quantum dot light-emitting diode (QD-LED) architecture featuring QDs sandwiched between an electron transport layer (ETL) and a hole transport layer (HTL). In addition to the presence of defect or surface states on QDs, which can result in an increase in the trap-assisted recombination rate ( $k_t$ ), the voltage and current required for LED operation results in an electric field on the QDs and charge, that, in turn, affects the radiative ( $k_r$ ) and non-radiative ( $k_{nr}$ ) recombination rates for excitons generated in the QD-LED.

results in an increase in  $k_{nr}$ , which, as seen in Equation 1, decreases the QY. Alternatively, the presence of charge on a QD, resulting from an improper balance of electron and hole injection, for example, can increase the Auger non-radiative recombination, where energy is dissipated as kinetic energy to a charge carrier instead of as a photon.<sup>8,9</sup> Again, this increases  $k_{nr}$  and decreases the QY.

In most QD-LEDs, the QD active layer also experiences an electric field on the order of 1 MV/cm. It has recently been shown, using a combination of experiment and theory, that in a QD, while  $k_{nr}$  is not affected by the electric field in the device, the electric field can induce a spatial separation of the electron and hole wave functions that is sufficient to significantly reduce the radiative rate of the exciton.<sup>10</sup> In the limit where  $k_r$  is smaller or on the order of  $k_{nr}$  ( $k_r \leq k_{nr}$ ), Equation 1 shows that a reduction of the radiative rate can cause a significant reduction in the EQE of the QD-LED.

**Designing QDs for LED applications**

Over the past 20 years, excellent progress has been made in the development of QD chemistries to improve the QY of the QD emitters. These chemistry advances can be broadly categorized into two trends: overcoating of the QD core with a shell material and grading the QD core composition, which is referred to as alloying.<sup>11</sup> As shown schematically in **Figure 2**, these modifications to the QD can result in a change in the degree of confinement of an exciton, in the extent of surface passivation, or a combination of these two effects. We discuss how these changes in QD chemistry have led to improvement of the QYs through a reduction of the non-radiative processes.

Starting with a CdSe core (upper left of Figure 2), the addition of a shell passivates the surface of a QD core and offers physical separation of the exciton from defect states on

the surface of the QD (right side of Figure 2). This results in a decrease in the non-radiative trap-assisted recombination rate ( $k_t$ ), thereby improving the luminescence QY of the QD.<sup>12-14</sup> This is highlighted by the recently developed “giant” shell CdSe/CdS QDs, where CdSe cores are overcoated with CdS such that the thickness of the shell is more than double the core diameter.<sup>15,16</sup> These QDs are reported to sustain a high degree of thermal stress and maintain their luminescence even when the passivating ligands are removed.

While the addition of a shell tends to consistently improve passivation of the QD, depending on the energy levels of the shell material relative to those of the core, the shell can either increase or decrease confinement of the exciton. For example, in a CdSe/ZnS QD, where a ZnS shell is added to a CdSe core as shown in the upper right of Figure 2, the wave functions of the electron (blue shading) and hole (red shading) that make up the exciton are more strongly spatially confined in the CdSe core due to the large energy offsets between the valence and conduction bands of the CdSe and ZnS. This increase in exciton confinement can be easily observed as shift of the emission in the QD to higher energies, as expected from a quantum mechanical particle-in-a-box picture. Specifically, a red-emitting CdSe QD that is overcoated with ZnS shell will emit in the green. This spatial confinement promotes strong carrier-carrier interactions, which results in the QDs retaining the high Auger non-radiative recombination rate ( $k_a$ ) of the core.<sup>8</sup>

In contrast, when a CdSe QD is overcoated with CdS (lower right of Figure 2), the hole wave function remains confined on the CdSe core, while the electron wave function extends into

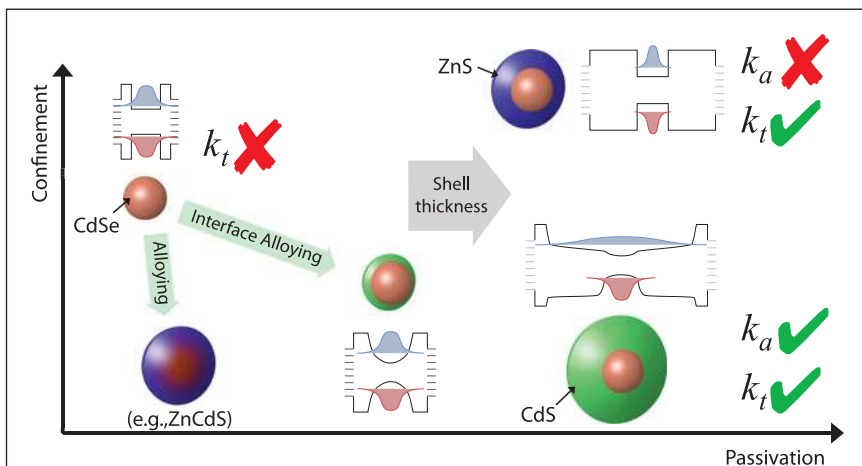


**Figure 2.** Schematic summarizing the positive (green check) or negative (red cross) impact a specific quantum dot (QD) structure has on the trap-assisted ( $k_t$ ) or Auger ( $k_a$ ) non-radiative recombination rate. QD structures are organized according to their extent of surface passivation and electronic confinement with respect to a CdSe core located in the upper left. Each QD structure is illustrated along with its energy band diagram showing the wave functions of the electron (blue) and hole (red).

the shell. This decrease in the electron confinement, which reduces carrier-carrier interactions, has been shown experimentally to decrease the Auger non-radiative recombination rate ( $k_a$ ).<sup>17,18</sup>

QDs with alloyed composition, such as ZnCdS or ZnCdSe, are also understood to have low  $k_a$ .<sup>19</sup> This has been explained theoretically by a smoothing of the shape of the confinement potential (see lower left of Figure 2) that is believed to occur in these alloyed QDs.<sup>20</sup> Alloying is also thought to be present at the core-shell interface in the “giant” shell QDs, which, in addition to the reduced electron confinement, can explain the observation of extremely low  $k_a$  in these QDs.<sup>20</sup>

Based on these considerations, it would seem that “giant” shell QDs, which offer the optimal passivation and reduction of Auger non-radiative recombination, would be the ideal choice for an emitter in a QD-LED. However, record efficiencies in QD-LEDs have not been reported with “giant” shell CdSe/CdS QD materials.<sup>21</sup> Instead, QD-LEDs with multilayered alloyed structures such as ZnCdS/ZnS, CdZnSe/CdZnS, or ZnCdSe exhibit the highest EQEs.<sup>3,22,23</sup> This can be understood by considering the impact of the electric field on the QY on the different types of QDs discussed previously.

As shown in **Figure 3a**, increasing the electric field across CdSe/CdS QDs decreases the luminescence QY.<sup>10</sup> The extent of the decrease, which can exceed a factor of 10 for electric fields encountered in a QD-LED, is dictated by the thickness of the CdS shell. Significantly less quenching is observed for a ZnS shell; however, it is still present and important for QD-LED efficiency.<sup>24</sup> Indeed, a recent study has shown that this field-induced luminescence quenching is responsible for the efficiency droop seen in EQE versus current density plots for many QD-LEDs.<sup>25</sup>

While electric field-induced luminescence quenching has been observed for QDs and other nanocrystal shapes<sup>26</sup> at both the single QD<sup>27,28</sup> and ensemble levels,<sup>29</sup> until recently,<sup>10,25</sup> no clear consensus was reached on its origins. As with Auger

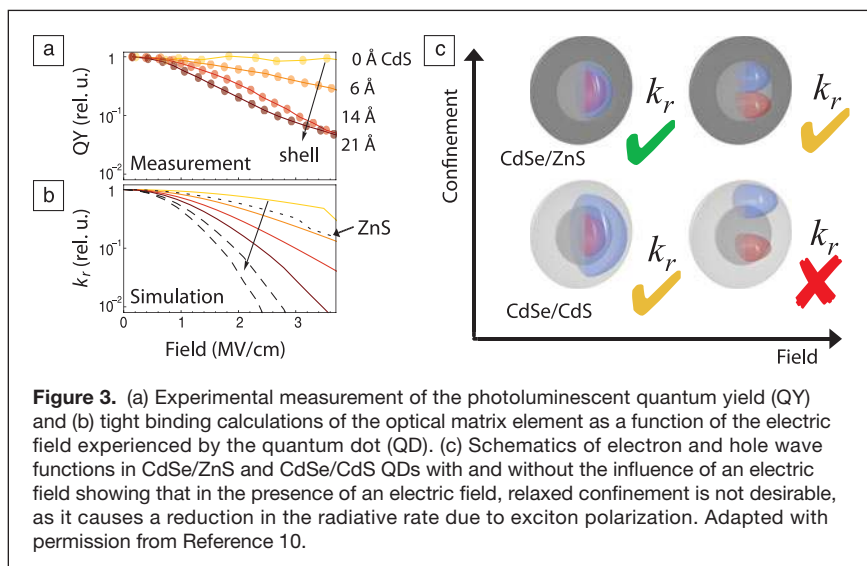
non-radiative recombination, the origins of field-driven luminescence quenching relate to QD band structure. Time-dependent photoluminescence measurements of the QDs exposed to varying electric fields reveal the exciton lifetime to be invariant with the field. This implies that the electric field does not change the non-radiative rate. Calculations of the optical matrix element (Figure 3b), which is proportional to the radiative rate ( $k_r$ ) and reflects the spatial overlap in the electron and hole wave functions, confirm that the decrease in luminescence QY can be assigned to a decrease in the radiative rate.<sup>10</sup> As illustrated schematically in Figure 3c, selecting a QD chemistry with decreased electronic confinement (e.g., a CdS shell instead of a ZnS shell for a CdSe core QD) allows for spatial separation of the electron and hole wave functions (blue and red shading) when the QD is exposed to an electric field. This effect can be referred to as exciton polarization and reduces the radiative recombination rate ( $k_r$ ).

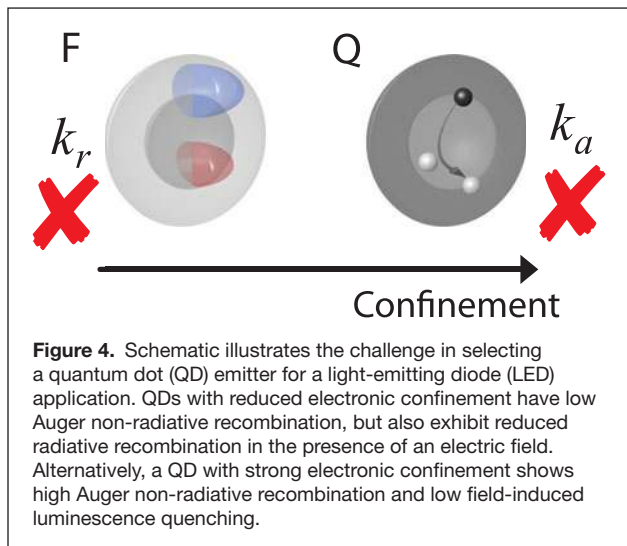
The previous discussion highlights the challenge in developing a QD for use as an emitter in a QD-LED, where the QDs are subject to both charge carriers and electric fields. The trade-off associated with choosing the optimal degree of exciton confinement that emerges from this discussion is depicted in **Figure 4**. A QD with minimal electronic confinement (left side of Figure 4) will likely not suffer from reduced QY even as charge accumulates on it during LED operation. However, this QD will experience increased electric field-induced luminescence quenching. Conversely, while a QD with a large confinement potential (right side of Figure 4) will not experience a significant loss in QY when exposed to an electric field, charging of the QD will decrease the QY and pose a significant challenge for high-performance QD-LED operation.

### Solutions for high-efficiency QD-LEDs

Design of the optimal QD emitter for a QD-LED is therefore non-trivial. Based on the previous consideration, a multilayered alloyed structure that offers (1) a core with a smoothed confinement potential to minimize Auger non-radiative recombination and (2) a shell that confines the electron and hole wave functions in the core so as to passivate the QD and minimize exciton polarization in an electric field seems to represent the optimal design for a QD emitter. However, such a QD structure can be a challenge to synthesize for all desired wavelengths. Furthermore, the specific band structure for each color-emitting QD in the QD-LED would need to be tailored to the local electric fields and charge distributions present at the QD during device operation.

Therefore, while it is possible to develop QD emitters that exhibit a high QY for a specific set of QD-LED operation conditions, in the following sections, we discuss design concepts that could be implemented at the level of the QD emitters, the active layer containing





the QDs, and the device structure that could at least partially ease the requirements of a highly optimized QD band structure.

**QD luminescence from localized states**

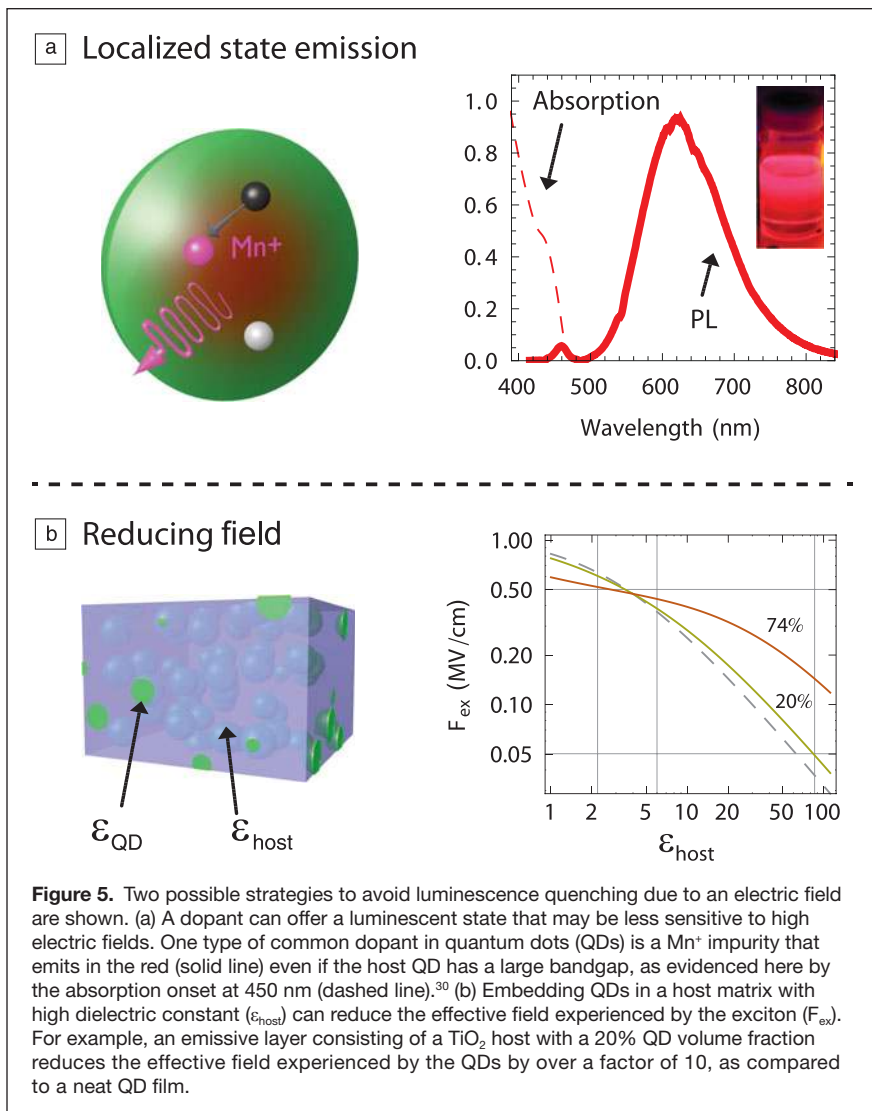
One strategy to improve upon QD emitters is to minimize field-induced luminescence quenching in QDs already exhibiting low Auger non-radiative recombination rates and high photoluminescence QYs. One scheme for this could be the rapid transfer of an exciton formed in an alloyed or thick-shelled QD to a localized state such that exciton polarization in the presence of an electric field is reduced. Such a scenario could be achieved through the introduction of a luminescent impurity such as  $Mn^{2+}$  into an alloyed QD (See **Figure 5a**) or through selection of a QD, such as  $CuInS_2$  or  $CuInSe_2$ , where luminescence occurs through a donor-acceptor process.<sup>30,31</sup>

**QD active layer placement and engineering**

Another approach to circumvent the limitations to EQE due to electric field-induced luminescence quenching is to minimize exposure of the QDs to high electric fields.

As a first step, this implies that QDs should be placed away from material interfaces, where electric fields are typically very high (~1 MV/cm). It has been shown that this strategy can significantly improve QD-LED EQE efficiencies.<sup>5</sup>

A different way to protect QDs from high electric fields is through their encapsulation in a high- $k$  host material, which could be carried out, for example, using chemical bath deposition<sup>32</sup> or atomic layer deposition in-filling of the QD active layer.<sup>33,34</sup> Using Maxwell-Garnett and Clausius-Garnett theory, we estimate how placement of the QDs in a host material with given dielectric constant,  $\epsilon_{host}$ , reduces the field ( $F_{ex}$ ) experienced by excitons on the QDs. To compare QD active layers with different  $\epsilon_{host}$ , we assume that the electric field in the QD-LED transport layers adjacent to the QD-host remains constant. This is equivalent to assuming a fixed displacement charge, which for normal QD-LED operation is roughly on the order of 0.2  $\mu C/cm^2$ , assuming 10 V bias over a 100-nm-thick device with a relative dielectric constant of 2.2. As shown in **Figure 5b**, we find that for low  $\epsilon_{host}$ , the field experienced by the exciton ( $F_{ex}$ ) is hardly influenced by the exact host dielectric constant or the volume fraction of the QDs. However, a high dielectric constant material such as  $TiO_2$  ( $\epsilon \geq 86$ ) can reduce the effective field by a factor of 10 for a QD volume fraction of 20%, which demonstrates the possibility for a significant alleviation of field-induced luminescence quenching.



### Novel device architectures and mechanisms for QD electroluminescence

Another option to reduce the challenges associated with designing a QD that exhibits high QY in the presence of both charge and electric field is to consider device architectures that are not *pn*-junctions and that achieve QD-electroluminescence in new ways. An example of such a device architecture, which highlights the possibility for a paradigm shift away from charge injection into QDs as a means for electroluminescence is an electric field-driven QD-LED.<sup>35</sup>

**Figure 6** shows a typical field-driven device structure where the emissive QD-containing layer is sandwiched between two insulating, wide bandgap oxide layers such as Al<sub>2</sub>O<sub>3</sub> or SiO<sub>2</sub>.<sup>36,37</sup> The device structure is completed with two electrodes. When a voltage is applied across the device, no charge is injected from the contacts into the QD layer; however, electroluminescence is still observed. As depicted in Figure 6, when the voltage applied across each QD exceeds its bandgap energy, an electron can transfer from the valence band of one QD to the conduction band of a neighboring QD (i.e., QD ionization), creating a spatially separated electron and hole in the QD film that can subsequently radiatively recombine.<sup>37</sup> Application of a pulsed applied electric field enables sustained electroluminescence in such a device. In addition to high-voltage pulsed operation of these capacitive devices, it is also possible to achieve field-driven electroluminescence in relatively low-voltage, constant current-driven devices by incorporation of thin (~15 nm thick) electron blocking layers

into the device, which permit sufficient buildup of an electric field to allow for the QD ionization process described previously.<sup>38</sup>

To study the mechanism of field-driven electroluminescence in detail, time-resolved luminescence studies were carried out while charge and electric field in the QD film were simultaneously measured.<sup>24,37</sup> It was found that following the ionization step, the applied electric field transports electrons and holes away from each other toward opposite QD/oxide interfaces. This redistribution of charges creates an internal electric field that screens the external applied field. When the external applied electric field is removed, the internal field, which is present due to the spatial separation of electron and hole populations, causes these electrons and holes to drift toward each other and recombine.

Therefore, despite the high electric fields on the order of 5 MV/cm needed to generate the free charge, luminescence in field-driven QD-LEDs occurs under lower electric field conditions (~1 MV/cm). This can be readily observed in Figure 6 from the lack of a pronounced red shift between the QD photoluminescence and electroluminescence spectra, which one would expect for QDs in high electric fields due to the Stark effect.<sup>27</sup> Furthermore, because electric field-driven luminescence is inherently a local process, the emissive layer need not be a continuous QD film, but could consist of clusters of QDs embedded within an insulating matrix. Indeed, field-driven electroluminescence has been demonstrated for high QY, QD-insulating polymer blends, which had previously been restricted to applications involving optical excitation of colloidal QDs.<sup>37</sup>

The field-driven QD-LED alleviates the band alignment considerations that typically dictate which emissive materials can be electrically excited using particular charge transport layers. As highlighted by the photographs and spectra in Figure 6, luminescent materials that have different chemistries and absolute energy level positions, and whose peak emission wavelengths span the visible to near-infrared regions, can all be excited within the same device structure. The first report of electroluminescence from a Mn<sup>+</sup>-doped QD material was also achieved in a field-driven QD-LED.<sup>39</sup>

While field-driven devices remove some of the design constraints associated with traditional QD-LEDs and emphasize the opportunity for new types of QD-LEDs, significant optimization of these devices is still needed. Engineering of the QD band structure and the emissive layer to minimize the electric fields needed for ionization and control of the charge distributions within the active layer following ionization will be critical in achieving high EQEs in field-driven QD-LEDs.

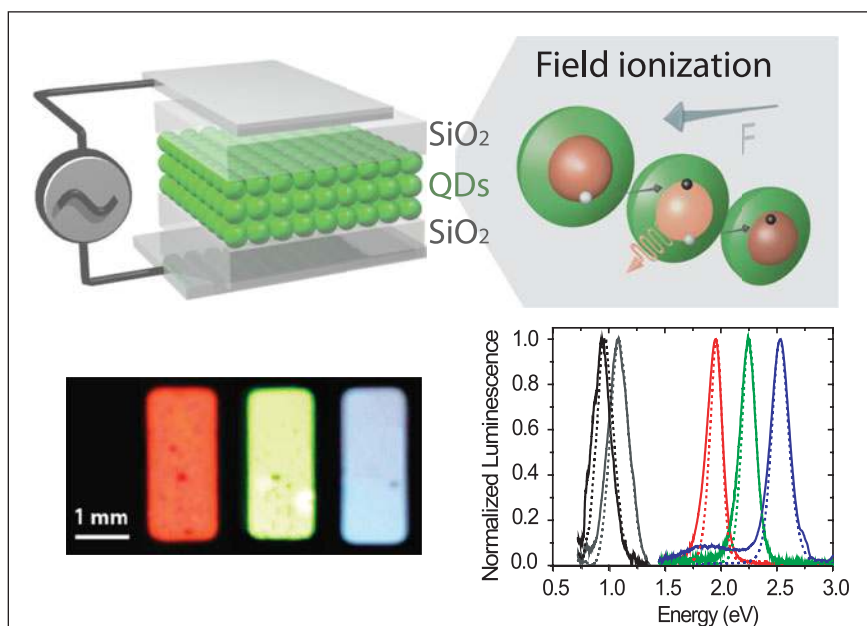


**Figure 6.** Schematics showing field-driven quantum dot light-emitting diode (QD-LED) device architecture and operating mechanism. Photographs of devices during operation and electroluminescence (EL) spectra (solid lines) show that different QDs can be excited within the same device structure. Comparison of the EL spectra to the photoluminescence spectra (dashed lines) of the QDs when the device is not in operation highlights that EL occurs at low electric field conditions. Adapted with permission from Reference 38. © 2011 American Chemical Society.

## Conclusion

The existence of both free charge carriers and electric fields in light-emitting diodes (LEDs) presents a challenge for the optimization of the quantum dot (QD) band structure. Thick-shelled QD emitters with reduced electronic confinement decrease Auger and trap-assisted non-radiative recombination, but they also exhibit decreased radiative recombination in the presence of an electric field. In contrast, core-shell QDs with strong confinement potentials show minimal luminescence quenching when subjected to electric fields, but suffer from high rates of Auger non-radiative recombination in the presence of charge. These phenomena explain in part why there are no electrically excited QD-LEDs commercially available today.

QDs consisting of alloyed cores with a smoothed confinement potential shape, which are further overcoated with shells, offer a solution to the design tradeoff. Additionally, selection of QDs exhibiting localized luminescence, placement of the QDs in a high dielectric host material, or adoption of field-driven QD-LED architectures serve as examples of potential innovations that address the challenges facing the realization of high-efficiency QD-LEDs. These solutions also bring novel design possibilities to QD-LED technologies, such as facile integration of non-Cd containing QD emitters and low cost, solution processable QD-metal oxide-based emissive thin films that could speed the development and commercialization of QD-LEDs for display and lighting applications.

## References

1. Y. Shirasaki, G.J. Supran, M.G. Bawendi, V. Bulović, *Nat. Photonics* **7**, 13 (2012).
2. B.S. Mashford, M. Stevenson, Z. Popovic, C. Hamilton, Z. Zhou, C. Breen, J. Steckel, V. Bulovic, M. Bawendi, S. Coe-Sullivan, P.T. Kazlas, *Nat. Photonics* **7**, 407 (2013).
3. P.O. Anikeeva, J.E. Halpert, M.G. Bawendi, V. Bulović, *Nano Lett.* **9**, 2532 (2009).
4. J. Kwak, W.K. Bae, D. Lee, I. Park, J. Lim, M. Park, H. Cho, H. Woo, D.Y. Yoon, K. Char, S. Lee, C. Lee, *Nano Lett.* **12**, 2362 (2012).
5. P. Anikeeva, C. Madigan, J. Halpert, M. Bawendi, V. Bulović, *Phys. Rev. B* **78**, 085434 (2008).
6. V. Wood, V. Bulović, *ACS Nano* **3**, 3581 (2009).
7. M. Kuno, J.K. Lee, B.O. Dabbousi, F.V. Mikulec, M.G. Bawendi, *J. Chem. Phys.* **106**, 9869 (1997).

8. V.I. Klimov, *Science* **287**, 1011 (2000).
9. C. Galland, Y. Ghosh, A. Steinbrück, M. Sykora, J.A. Hollingsworth, V.I. Klimov, H. Htoon, *Nature* **479**, 203 (2011).
10. D. Bozyigit, O. Yarema, V. Wood, *Adv. Funct. Mater.* **23**, 3024 (2013).
11. D.V. Talapin, J.-S. Lee, M.V. Kovalenko, E.V. Shevchenko, *Chem. Rev.* **110**, 389 (2010).
12. M.A. Hines, P. Guyot-Sionnest, *J. Phys. Chem.* **100**, 468 (1996).
13. B.O. Dabbousi, J. Rodriguez-Viejo, F.V. Mikulec, J.R. Heine, H. Mattoussi, R. Ober, K.F. Jensen, M.G. Bawendi, *J. Phys. Chem. B* **101**, 9463 (1997).
14. O. Chen, J. Zhao, V.P. Chauhan, J. Cui, C. Wong, D.K. Harris, H. Wei, H.-S. Han, D. Fukumura, R.K. Jain, M.G. Bawendi, *Nat. Mater.* **12**, 445 (2013).
15. B. Mahler, P. Spinicelli, S. Buil, X. Quelin, J.P. Hermier, B. Dubertret, *Nat. Mater.* **7**, 659 (2008).
16. Y. Chen, J. Vela, H. Htoon, J.L. Casson, D.J. Werder, D.A. Bussian, V.I. Klimov, J.A. Hollingsworth, *J. Am. Chem. Soc.* **130**, 5026 (2008).
17. F. García-Santamaría, Y. Chen, J. Vela, R.D. Schaller, J.A. Hollingsworth, V.I. Klimov, *Nano Lett.* **9**, 3482 (2009).
18. F. Garcia-Santamaría, S. Brovelli, R. Viswanatha, J.A. Hollingsworth, H. Htoon, S. Crooker, V.I. Klimov, *Nano Lett.* **11**, 687 (2011).
19. X. Wang, X. Ren, K. Kahen, M.A. Hahn, M. Rajeswaran, S. Maccagnano-Zacher, J. Silcox, G.E. Cragg, A.L. Efros, T.D. Krauss, *Nature* **459**, 686 (2009).
20. G.E. Cragg, A.L. Efros, *Nano Lett.* **10**, 313 (2010).
21. B.N. Pal, Y. Ghosh, S. Brovelli, R. Laocharoensuk, V.I. Klimov, J.A. Hollingsworth, H. Htoon, *Nano Lett.* **12**, 331 (2012).
22. J.S. Steckel, P. Snee, S. Coe-Sullivan, J.P. Zimmer, J.E. Halpert, P. Anikeeva, L.-A. Kim, V. Bulović, M.G. Bawendi, *Angew. Chem.* **45**, 5796 (2006).
23. J.M. Caruge, J.E. Halpert, V. Wood, V. Bulović, M.G. Bawendi, *Nat. Photonics* **2**, 247 (2008).
24. D. Bozyigit, V. Wood, Y. Shirasaki, V. Bulović, *J. Appl. Phys.* **111**, 113701 (2012).
25. Y. Shirasaki, G.J. Supran, W.A. Tisdale, V. Bulović, *Phys. Rev. Lett.* **110**, 217403 (2013).
26. R. Kraus, P.G. Lagoudakis, A.L. Rogach, D.V. Talapin, H. Weller, J.M. Lupton, J. Feldmann, *Phys. Rev. Lett.* **98**, 3 (2007).
27. S.A. Empedocles, *Science* **278**, 2114 (1997).
28. S.-J. Park, S. Link, W.L. Miller, A. Gesquiere, P.F. Barbara, *Chem. Phys.* **341**, 169 (2007).
29. M. Jarosz, V. Porter, B. Fisher, M. Kastner, M. Bawendi, *Phys. Rev. B* **70**, 195327 (2004).
30. R. Thakar, Y. Chen, P.T. Snee, *Nano Lett.* **7**, 3429 (2007).
31. D. Aldakov, A. Lefrançois, P. Reiss, *J. Mater. Chem. C* **1**, 3756 (2013).
32. E. Kinder, P. Moroz, G. Diederich, A. Johnson, M. Kirsanova, A. Nemchinov, T. O'Connor, D. Roth, M. Zamkov, *J. Am. Chem. Soc.* **133**, 20488 (2011).
33. Y. Liu, M. Gibbs, C.L. Perkins, J. Tolentino, M.H. Zarghami, J. Bustamante, M. Law, *Nano Lett.* **11**, 5349 (2011).
34. A. Pourret, P. Guyot-Sionnest, J.W. Elam, *Adv. Mater.* **21**, 232 (2009).
35. V. Wood, V. Bulović, *Nano Rev.* **1** (2010), doi:10.3402/nano.v1i0.5202.
36. S. Kobayashi, Y. Tani, H. Kawazoe, *Jpn. J. Appl. Phys.* **46**, L966 (2007).
37. V. Wood, M.J. Panzer, D. Bozyigit, Y. Shirasaki, I. Rousseau, S. Geyer, M.G. Bawendi, V. Bulović, *Nano Lett.* **11**, 2927 (2011).
38. V. Wood, M.J. Panzer, J.-M. Caruge, J.E. Halpert, M.G. Bawendi, V. Bulović, *Nano Lett.* **10**, 24 (2010).
39. V. Wood, J.E. Halpert, M.J. Panzer, M.G. Bawendi, V. Bulović, *Nano Lett.* **9**, 2367 (2009). □

**2014 MRS**  
**SPRING MEETING & EXHIBIT**  
 April 21-25, San Francisco, CA



**CALL FOR PAPERS**

**Abstract Deadline • November 1, 2013**  
 Abstract Submission Site Opens • October 1, 2013  
[www.mrs.org/spring2014](http://www.mrs.org/spring2014)

- ENERGY
- SOFT AND BIOMATERIALS
- ELECTRONICS AND PHOTONICS

- NANOMATERIALS
- GENERAL—THEORY AND CHARACTERIZATION
- EDUCATION/MENTORING SYMPOSIUM